

# Simultaneous extraction of Diffusion length and Surface recombination velocity from an EBIC line scan using Artificial Neural Networks

<sup>1</sup>*Souhila Soualmia*

<sup>1</sup>*Department of Physics, Batna University, Batna, Algeria*

## Abstract

The performance and functionality of semiconductor devices is directly affected by the transport properties of carriers. In this work, we develop a novel and effective approach for the simultaneous extraction of the *diffusion length*  $L$  and the *normalized surface recombination velocity*  $S$ , from the same Electron Beam Induced Current (EBIC) as a function of beam position in a normal-collector configuration. The approach is based on feedforward artificial neural network (ANN), where the ANN is trained to learn the relationship between the input of the system (*diffusion length / surface recombination velocity*) and the output of the system (EBIC). After training the ANN, it is possible to observe the reverse process and extract *the diffusion length / the surface recombination velocity* from any EBIC current using an exhaustive search method. An optimum set of values is obtained with an error less than 1.7% for the diffusion length and less than 4% for the normalized surface recombination velocity in 95% of the cases, and an error less than 2.7% for the diffusion length and less than 8% for the normalized surface recombination velocity in 100% of the cases.

**Keywords:** EBIC, parameter extraction, neural networks, diffusion length, surface recombination velocity.

**Full length article** \*Corresponding Author, e-mail: [ssoualmia.bb@gmail.com](mailto:ssoualmia.bb@gmail.com)

## 1. Introduction

The *Scanning electron microscopy* SEM is an important tool for the study and analysis of different specimens; it permits the observation and characterization on a *nanometer to micrometer* scale. It is one of the widely used techniques in research and industry [1-4]. In scanning electron microscopy, Electron Beam Induced Current (EBIC) is one of the most used tools for the investigation of crystal defects in semiconductors [5-9], and for the extraction of defect free region semiconductor parameters such as: the diffusion length ( $L$ ), and the normalized surface recombination velocity ( $S$ ) [10-20]. The parameter extraction problem is a multi-minimum optimization problem. Optimization algorithms tend to adjust the inputs such that the *cost function*, also known as the *objective function*, is either minimized or maximized (depending on whether it is a minimization or a maximization problem). One of the largest problems in optimization is to determine whether the solution found is a *global solution* (corresponds to finding the *global minimum/maximum*) or a *suboptimum solution* (corresponds to finding a *local minimum/maximum*) [21-24].

Artificial Neural Networks (ANN) are widely used in parameter extraction of semiconductor devices and Soualmia ., 2021

integrated circuits [25-33]; this is due to their specific characteristics such as their ability to learn by examples through training, their ability to generalize and predict, and their inherent parallel computation capability. In this work, a novel approach is developed for the simultaneous extraction of related semiconductor parameters: diffusion length  $L$  and surface recombination velocity  $S$ , from any EBIC signal of a defect free semi-infinite semiconductor. The approach is based on feedforward artificial neural networks; basically, an ANN is trained to learn the inherent relationship between the input parameters ( $L, S$ ) and the output parameter (EBIC signal versus electron beam position). Once the ANN has been trained, it is possible to observe the reverse process and extract the two parameters using an exhaustive search method.

Compared to other methods in the literature this approach has specific characteristics such as: (1) it is independent of the theoretical model (uses directly the data: experimental/simulation/theoretical, for training). (2) It is capable to generalize and extract any parameters from data not seen before. (3) finding the optimum values for the parameters ( $\alpha, L, S, Z_t, Q$ ) is guaranteed since the whole search space is scanned.

## 2. Electron Beam Induced Current

When a semiconductor sample is bombarded with an electron beam in a scanning electron microscope (SEM), electron-hole pairs are generated in the semiconductor bulk. When the semiconductor sample contains internal electric field (p-n junction or Schottky junction), the charge carriers are separated by that field and minority carriers can therefore reach the junction by diffusion; this results in a charge-collection current or electron beam induced current EBIC, which can be amplified and measured externally. Different geometries for observing EBIC are used [34]; the most commonly used one is the normal collector illustrated schematically in figure 1, which uses a p-n junction perpendicular to the electron beam incident surface. In figure 1,  $X_b$  represents the distance between the junction and the electron beam position.

When the presence of the back surface of the diode can be neglected (sample thickness considered infinite), the transport of the minority carriers generated by the electron beam in the neutral material (n type) is described by the following steady state diffusion equation [35]:

$$D_p \nabla^2 p(r) - \frac{p(r)}{\tau} + g(r) \dots \dots \dots (1)$$

Where  $p(r)$  is the excess hole density at the point  $r$ ,  $D_p$  and  $\tau$  are their diffusion coefficient and lifetime, respectively,  $g(r)$  is the generation rate of the electron hole pairs per unit volume.

The boundary conditions are [35]:

$$p = 0 \quad \text{at} \quad x = 0 \quad \dots \dots \dots (2a)$$

$$\frac{\partial p}{\partial z} = S.p \quad \text{at} \quad z = 0 \quad \dots \dots \dots (2b)$$

Where  $S = V_s / L D$  is the normalized surface recombination velocity, where  $V_s$  is the surface recombination velocity and  $V_d$  is the diffusion velocity ( $V_d = L / \tau$ ).

The EBIC current is calculated in the three regions:  $n$  region, the depletion layer region, and the  $p$  region, as follows [36,37]:

$$I(x') = \int_0^{\infty} \int_{-\infty}^{x_n} g_{xz}(x-x', z) i(x, z) dx dz + \int_0^{\infty} \int_{x_n}^{x_p} g_{xz}(x-x', z) dx dz + \int_0^{\infty} \int_0^{x_p} g_{xz}(x-x', z) i(x, z) dx dz \dots \dots \dots (3)$$

Where  $x_p$  and  $x_n$  are the edges of the depletion layer,  $g_{xz}(x, z)$  is the projected generation onto the  $xz$  plane (since the contribution to the collected current does not depend on the  $y$  coordinate), and is given by [35]:

$$g_{xz}(x, z) = \int_{-\infty}^{\infty} g(x, y, z) dy \dots \dots \dots (4)$$

And:

$$i(x, z) = \exp(-\lambda x) - \frac{2S}{\pi} \int_0^{\infty} \frac{k}{\mu^2(\mu + S)} \exp(-\mu z) \sin(kx) dk \dots \dots \dots (5)$$

is the induced current due to a point source located in  $(x, z)$  [35] and  $k$  is a constant,  $\lambda = 1/L$ ,  $\mu = (\lambda^2 + k^2)^{1/2}$ .

The EBIC current versus the beam position for different values of the diffusion length  $L$  and different values of the surface recombination velocity  $S$  is presented in figure 2. The sample material is silicon and the energy beam is equal to 3KeV.

## 3. Parameter extraction algorithm

### 3.1. Parameter extraction as an optimization problem

The parameter extraction problem can be formulated as an optimization problem where the objective function given by  $E(\mathbf{x}) = E(\mathbf{y}' - f(\mathbf{x}))$  is minimized. Here,  $\mathbf{y} = f(\mathbf{x})$  is a process with output  $\mathbf{y}$  and input  $\mathbf{x}$ , where  $x$  is subject to the constraint  $\mathbf{C}$ . The output  $\mathbf{y}'$  is a sample output measurement and the operator  $E$  is a general error operator (in our case we use the Euclidean distance), By solving this optimization problem, our goal is to find the input  $x^*$  such that:

$$\mathbf{x}^* = \underset{\substack{\mathbf{x} \\ \text{subject to } \mathbf{C}}}{\text{arg min}} (E(\mathbf{x})) \dots \dots \dots (6)$$

In the ensuing, we detail the different steps involved in the parameter extraction process. The process consists of six steps as shown in table 1.

In the following, we provide more details about the above-mentioned steps.

### 3.2. Data sets Preparation:

- In this step, the parameters  $L$  and  $S$  are sampled and arranged into vectors, that is:  $\mathbf{L}^{train} = [L_1^{train}, L_2^{train}, \dots, L_m^{train}]$ , and  $\mathbf{S}^{train} = [S_1^{train}, S_2^{train}, \dots, S_n^{train}]$ , with dimensions  $\{1\text{-by-}m\}$ , and  $\{1\text{-by-}n\}$ , respectively. Then, the input training matrix  $\mathbf{X}^{train}$  of dimension  $\{2\text{-by-}m \times n\}$  is formed by taking all possible combinations of vectors  $\mathbf{L}^{train}$ ,  $\mathbf{S}^{train}$ . Finally, the output training matrix  $\mathbf{Y}^{train}$  is obtained for each column of  $\mathbf{X}^{train}$  by using Donolato's model to calculate the EBIC signal for different values of the beam position.
- For the test data set, the parameters  $L$  and  $S$  are also sampled and arranged into vectors, but this is done by considering the mid-value between each two consecutive values of the training vectors as follows:  $\mathbf{L}^{test} = [L_1^{test}, L_2^{test}, \dots, L_{m-1}^{test}]$  and  $\mathbf{S}^{test} = [S_1^{test}, S_2^{test}, \dots, S_{n-1}^{test}]$ . These vectors have dimensions of  $\{1\text{-by-}(m-1)\}$ , and  $\{1\text{-by-}(n-1)\}$ , respectively. Again, input test matrix  $\mathbf{X}^{test}$  of dimension  $\{2\text{-by-}(m-1) \times (n-1)\}$  is obtained by

taking all possible combinations of  $\mathbf{L}^{test}$  and  $\mathbf{S}^{test}$ . The output test matrix is for each column of the matrix  $\mathbf{X}^{test}$  is calculated using Donolato's model.

### 3.3. ANN training

The aim of this step is train the ANN to learn the relationship between the input data  $\mathbf{X}^{train}$  and the output data  $\mathbf{Y}^{train}$ , that is:

$$\mathbf{X}^{train} \xrightarrow{f} \mathbf{Y}^{train} \dots \dots \dots (7)$$

, The input data set  $\mathbf{X}^{train}$  is fed to the ANN and used to calculate the actual output data set  $\mathbf{Y}^{actual}$ . The latter is subtracted from the desired output data set  $\mathbf{Y}^{train}$  yielding an error  $\mathbf{e}$ . This error is then used for ANN weights updating. This procedure is repeated a number of times till the sum squared error (SSE) drops below a certain threshold. This is illustrated in figure 3

The SSE is given by the following equation [27]:

$$SSE = \sum_{j=1}^{k^{train}} (Y_j^{train} - Y_j^{actual})^2 \dots \dots \dots (8)$$

where  $k^{train}$  designates the number of samples of  $\mathbf{Y}^{train}$ .

### 3.4. ANN Testing

In this step, the ability of the ANN to generalize is tested through the application of a new set of input values  $\mathbf{X}^{test}$  not seen before. The EBIC signal obtained from this step  $\tilde{\mathbf{Y}}^{test}$  is then compared to the desired EBIC signal  $\mathbf{Y}^{test}$ . Sample-by-sample percentage error between  $\mathbf{Y}^{test}$  and  $\tilde{\mathbf{Y}}^{test}$  is then taken using the following formula [27]:

$$e_{i,j} = \left| \frac{Y_{i,j}^{test} - \tilde{Y}_{i,j}^{test}}{Y_{i,j}^{test}} \right| \times 100 \dots \dots \dots (9)$$

where  $i$  and  $j$  designates the  $i^{th}$  row,  $j^{th}$  column of the matrices  $\mathbf{Y}^{test}$  and  $\tilde{\mathbf{Y}}^{test}$ , respectively.

### 3.5. EBIC signal Oversampling

In this step, the ability of ANNs to generalize is used to oversample (generate more samples) () the EBIC signal. This is done with low cost compared to the case where this is done by experimentation. Here as well, the EBIC signal  $\tilde{\mathbf{Y}}^{over}$  is calculated by ANN and compared to the desired data output  $\mathbf{Y}^{over}$  and sample-by-sample percentage error between  $\mathbf{Y}^{over}$  and  $\tilde{\mathbf{Y}}^{over}$  is obtained using equation (9). The input data matrix  $\mathbf{X}^{over}$  in this case is obtained by oversampling the vectors of the training data vectors  $\mathbf{L}^{train}$ ,  $\mathbf{S}^{train}$  and taking all possible combinations.

### 3.5. Parameter Extraction

In this step, the parameter extraction is performed using exhaustive search. This is done as follows: a database is created from the oversampled input data matrix  $\mathbf{X}^{over}$  and the oversampled output data matrix  $\tilde{\mathbf{Y}}^{over}$  and is used for the exhaustive search. After that, we consider a random EBIC curve  $\mathbf{y}^{rand}$  that can be obtained, for example from an experiment, is used to calculate the Euclidian distance between the latter and all other columns of matrix  $\tilde{\mathbf{Y}}^{over}$ . The values of the parameters  $L$  and  $S$  corresponding to the column of matrix  $\tilde{\mathbf{Y}}^{over}$  with the smallest Euclidian distance are considered as the extracted parameters, that is:

$$\arg \min_{j=1,2,\dots,K^{over}} \|\mathbf{y}^{rand} - \tilde{\mathbf{Y}}_j^{over}\|_2 \dots \dots \dots (10)$$

where  $K^{over}$  is the number of columns of  $\tilde{\mathbf{Y}}^{over}$ .

## 4. Simulation results

In this section we evaluate the performance of the proposed parameter extraction algorithm. We first start with the collection of the input/output data that will be used to train the ANN. In our work we consider Donolato's model to generate the input/output data [35] using the normal-collector configuration described previously (§ 2-2). Nevertheless, other approaches such as conducting Monte Carlo simulations or performing experimentations, can be used as well to form the input/output data for ANN training. The material sample considered in this work is Silicon and the electron beam is perpendicular to the surface of the semiconductor sample. The line scans the region outside the junction, and the energy beam is taken as 14 KeV which results in an energy range of 1.7  $\mu\text{m}$ .

### 4.1. Training algorithm

As mentioned before, during the training of the ANN, the EBIC signal is calculated for all combinations of parameters  $\mathbf{L}^{train}$  and  $\mathbf{S}^{train}$ . The values of  $\mathbf{L}^{train}$ ,  $\mathbf{S}^{train}$  are obtained from [36,37]. Table 2 depicts the values of these parameters.

As shown in table 2, considering all possible combinations of  $\mathbf{L}^{train}$ ,  $\mathbf{S}^{train}$  yields a total number of 2077 samples, all of which are used for training the ANN.

In this work, we consider a feed forward neural network that consists of one hidden layer, that comprises 5 neurons and uses logarithmic sigmoid transfer functions. The output layer consists of 5 neurons (corresponding to the number of parameters) and uses linear transfer functions. Table 3 depicts the ANN parameters used in this work.

As shown in Figure 4, the desired goal was attained after 40 epochs of training.

As depicted in Figure 5, the maximal percentage error between the theoretical training EBIC and the EBIC

calculated by the ANN for five values of the beam position is 0.9037%. This proves the successfulness of the training phase of the ANN.

We consider also, the histogram plot in figure 6. It is easy to see that most of the errors are clustered around zero, which indicates that the ANN is learning the input/output relationship effectively. The results are collected in table 4. which shows that the maximal error in 95% of the training samples is 0.4% only and the maximal error in 100% of the training samples is 1.2% only.

**4.2. Testing data**

Next, we test the trained ANN using values of EBIC signal not seen before as shown in table 5.

The number of testing samples used is 2010 samples. Figure 7 depicts the percentage error obtained by taking the difference between the samples of the test EBIC and the EBIC calculated by ANN. The maximum percentage error obtained is 1.5571%.

Also, the histogram plot of the error is depicted in figure 8. The results from figure 8, are summarized in table 6.

**4.3. Oversampling of EBIC signal**

As mentioned before, the oversampling of the input parameters is done by taking more samples between consecutive training samples, which are then used to generate the oversampled EBIC signal using the trained and tested ANN. The values of the different parameters used in this part are shown in table 7. Here, the number of input data samples used to oversample the EBIC signal is 10769.

As shown in Figure 9, the maximal percentage error is 0.9654%. To have a better idea about the performance of the ANN, the histogram of the error is also plotted in figure 10. The results of figure 10 are summarized in table 8. It is easy to see that the maximal error in 95% of the samples is 0.45% and the maximal error in 100% of the samples is 1.26%.

**4.4. Exhaustive search**

After oversampling the EBIC signal using the trained and tested ANN, an exhaustive search process is conducted to determine the value of the input parameters corresponding to the oversampled EBIC signal that is closest (in terms of Euclidian distance) to the EBIC signal under test. for which the input parameters are sought.

To quantify the the performance of the parameter extraction algorithm, we consider a large set of randomly selected EBIC curves with known input parameters ( $L, S$ ),. The percentage error between the true input parameter (nominal value) and the parameter determined using the proposed parameter extraction algorithm is given by:

$$e_{i,j} = \left| \frac{\mathbf{X}_{i,j}^{rand} - \mathbf{X}_{i,j}^{over}}{\mathbf{X}_{i,j}^{rand}} \right| \times 100 \dots \dots \dots (11)$$

and is calculated for each randomly selected EBIC curve.

In this part, 10680 randomly selected EBIC curves are used for testing the exhaustive search process. Figure 11 depicts the histogram and the CDF plots of the percentage error for each parameter. Results of figure 11, are summarized in table 9; the error is less than 8% in all cases and less than 4% in 95% of the cases. These results clearly illustrate the successfulness of the parameters extraction algorithm considered in this paper.

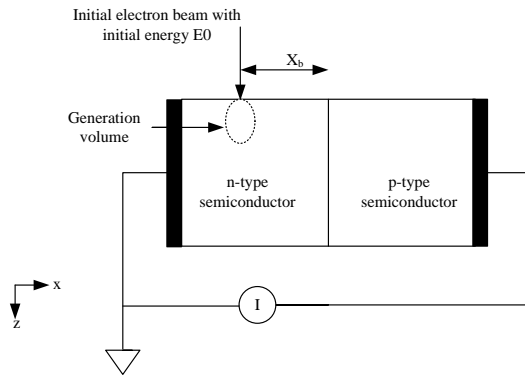


**Fig. 1** Schematic illustration of normal collector set up

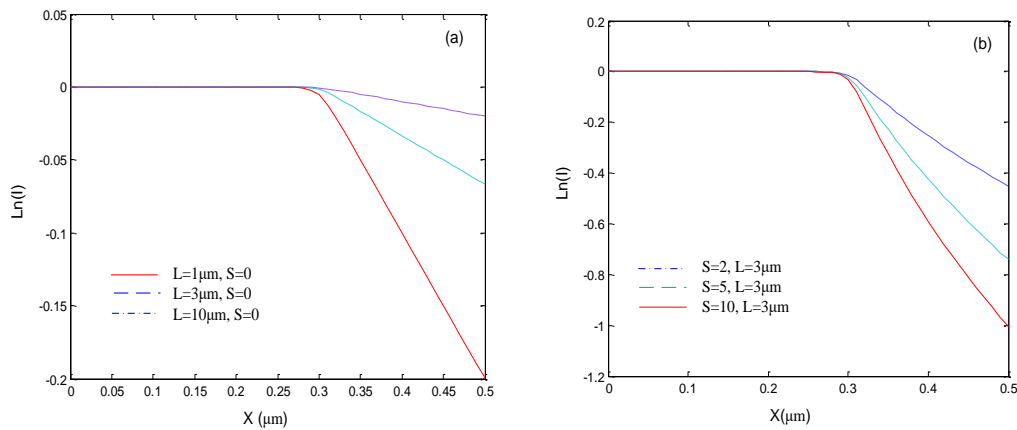


**Fig. 2** EBIC profiles for the region around the edges of a depletion layer located at  $0.3 \mu m$ : (a) different values of the diffusion length  $L$  ( $S=0$ ), (b) different values of the surface recombination velocity ( $L=3 \mu m$ ) (Same values as in [36,37] where taken)

**Table 1** Parameter extraction algorithm

Step	Process
1	Prepare training values of the two parameters $L$ and $S$ (training input of the system)
2	Using donolato's model, Calculate the EBIC signal, for different values of the energy beam (training output of the system).
3	Prepare test values of the two parameters $L$ and $S$ by taking mid values between two successive training data values (test input of the system).
4	Using donolato's model, Calculate the EBIC signal, for different values of the energy beam (test output of the system).
5	Train the ANN using input and output training data prepared in steps 1 and 2.
6	Test the ANN performance using the input and output test data prepared in steps 3 and 4.
7	Oversample the EBIC signal using the generalization property of ANNs
8	Extract the set of input parameters corresponding to a certain EBIC signal using exhaustive search

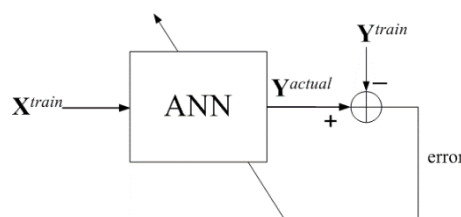


**Fig. 3** ANN learning procedure

**Table 2** Semiconductor parameters used for training

<i>Material Parameter</i>	<i>Minimal value</i>	<i>Maximal value</i>	<i>Sampling step size</i>	<i>Number of</i>
Beam position( $\mu m$ )	6	6.9	0.2	5
Diffusion length $L^{train}(\mu m)$	3	3.9	0.03	31
Normalized surface recombination velocity $S^{train}(\mu m^{-1})$	2	4	0.03	67
Total number of samples used for training	31×67=2077			

**Table 3** ANN parameters used for training

<i>ANN parameters</i>	
Number of epochs	300
Desired goal	$10^{-6}$
Number of hidden layers	1
Number of neurons in the hidden layer	5 uses logarithmic sigmoid transfer functions
Number of neurons in the output layer	5 (number of samples of the beam position) uses linear transfer functions

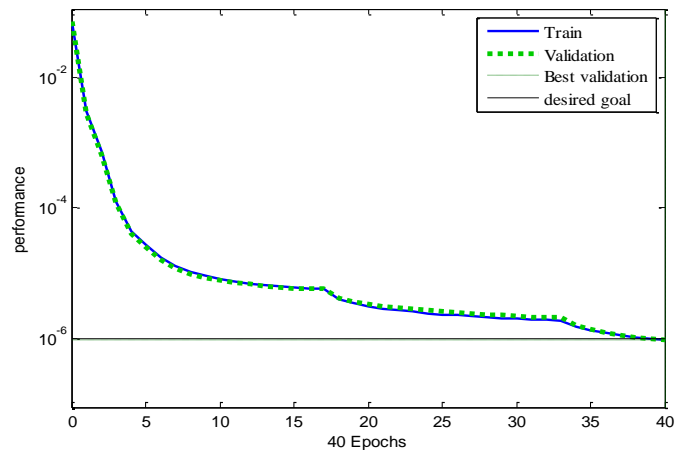


**Fig. 4** Training curve of the ANN

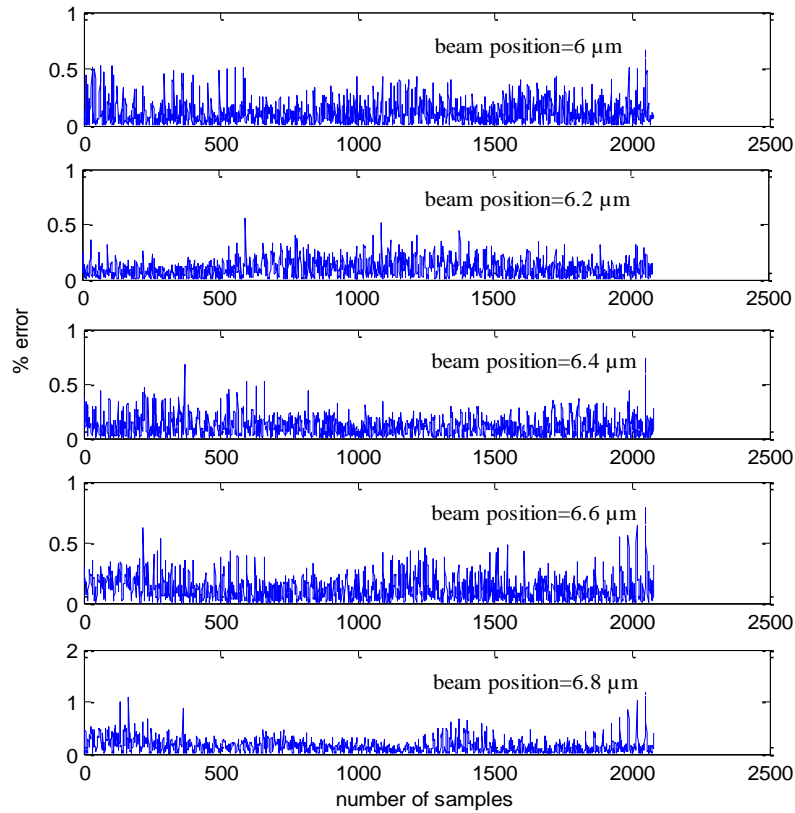


**Fig. 5** Percentage error between theoretical training EBIC signal and the training EBIC signal calculated by ANN

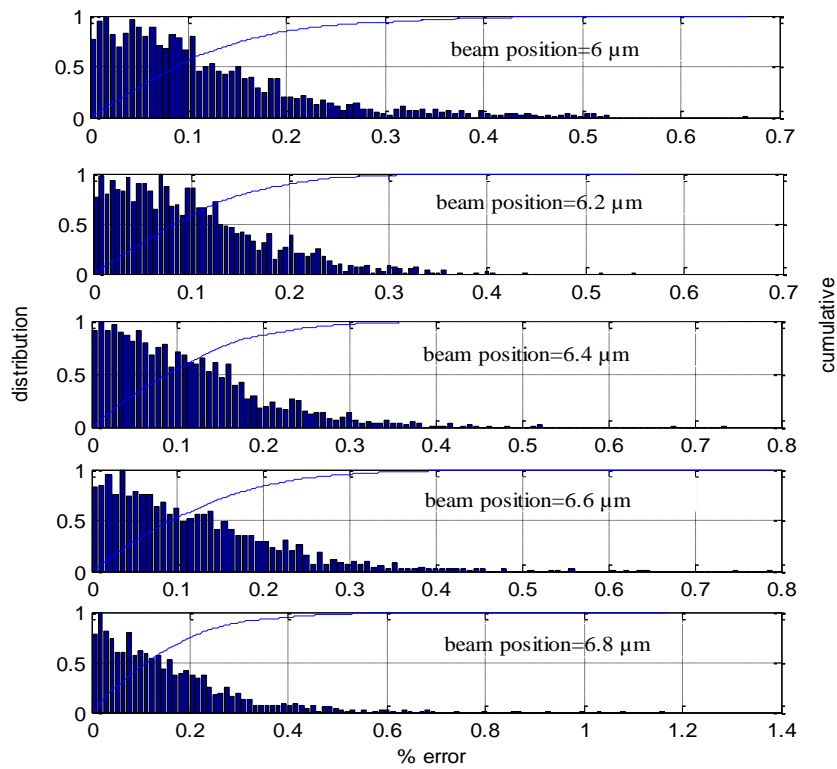


**Fig. 6** Probability density function (PDF) (bars) and cumulative distribution function (CDF) (solid line) of the percentage error for the training set

**Table 4** Error for 95% and 100% of the samples

Beam position value( $\mu\text{m}$ )	For 95% of the samples, error is below	For 100% of the samples, error is below
6	0.3%	0.65%
6.2	0.25%	0.55%
6.4	0.3%	0.75%
6.6	0.3%	0.8%
6.8	0.4%	1.2%

**Table 5** Semiconductor parameters used for testing the ANN

Material Parameter	Minimal value	Maximal value	Sampling step size	Number of samples
Beam position( $\mu\text{m}$ )	6	6.9	0.2	5
Diffusion length $L^{test}(\mu\text{m})$	$3+(0.03/2)$	3.9	0.03	30
Normalized surface recombination velocity $S^{test}$	$2+(0.03/2)$	4	0.03	67
Total number of samples for the test	$30 \times 67 = 2010$			

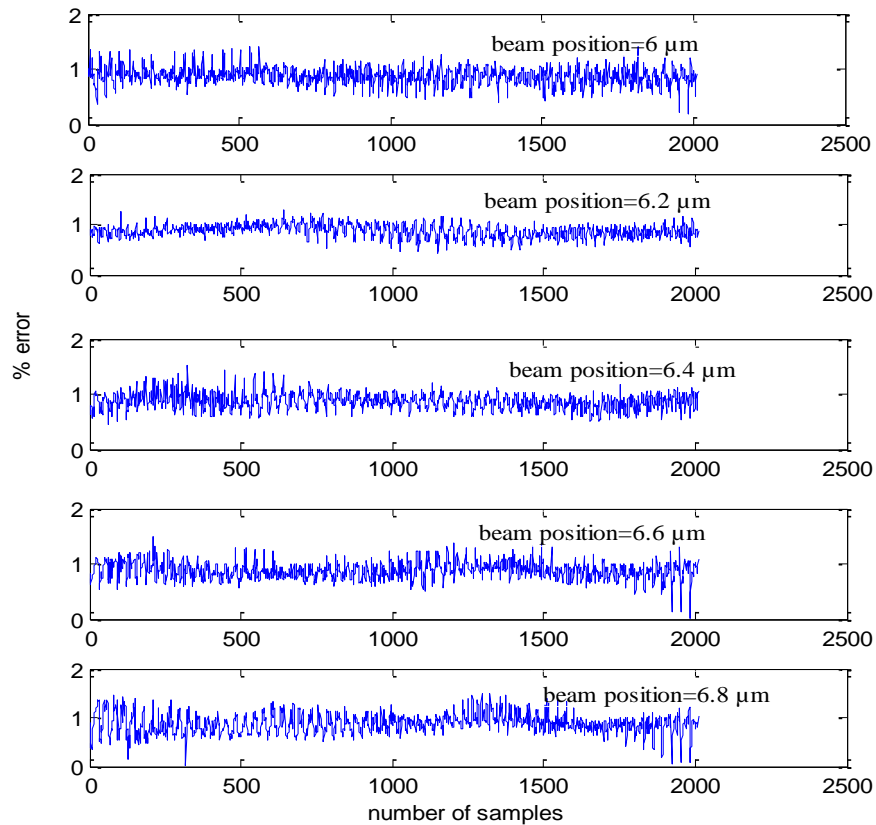


**Fig. 7** Percentage error between the theoretical test EBIC and the test EBIC calculated by ANN



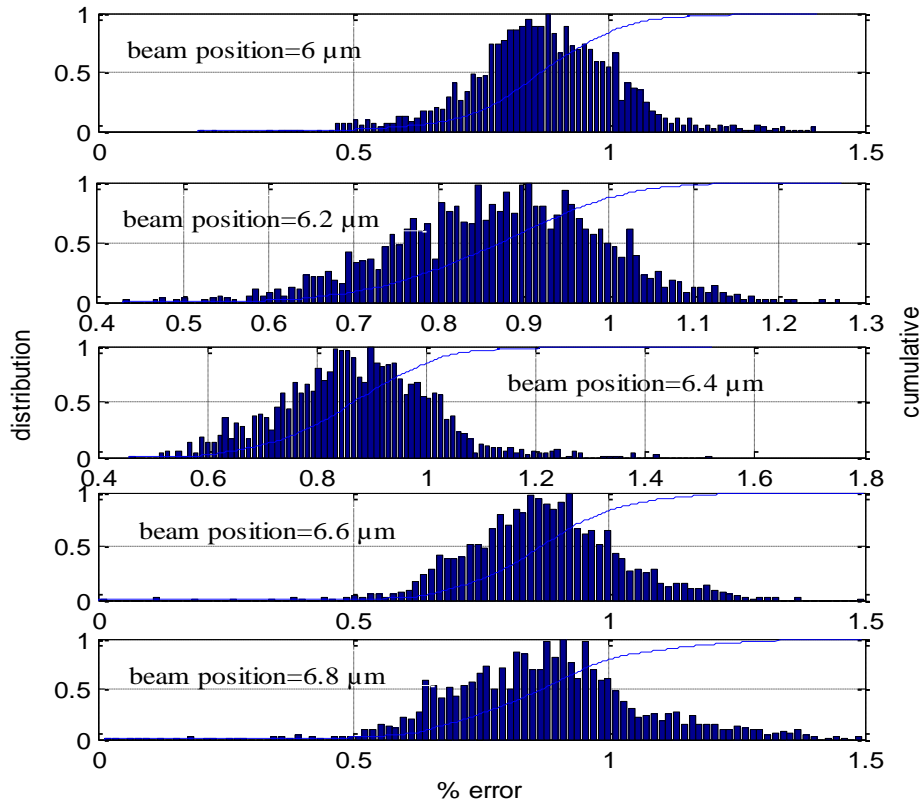


**Fig. 8** PDF and CDF of the percentage error for the test set

**Table 6** Error for 95% and 100% of the samples

<i>Beam position value(<math>\mu\text{m}</math>)</i>	<i>For 95% of the samples, error is below</i>	<i>For 100% of the samples, error is below</i>
6	1.08%	1.4%
6.2	1.04%	1.3%
6.4	1.1%	1.5%
6.6	1.1%	1.5%
6.8	1.2%	1.5%

**Table 7** Semiconductor parameters used to obtain the oversampled EBIC

<i>Material Parameter</i>	<i>Minimal value</i>	<i>Maximal value</i>	<i>Sampling step size</i>	<i>Number of samples</i>
Beam position ( $\mu\text{m}$ )	6	6.9	0.2	5
Diffusion length $L^{over}(\mu\text{m})$	3	3.9	0.03/4	121
Normalized surface recombination velocity	2	2.66	0.03/4	89
Total number of samples	121×89=10769			

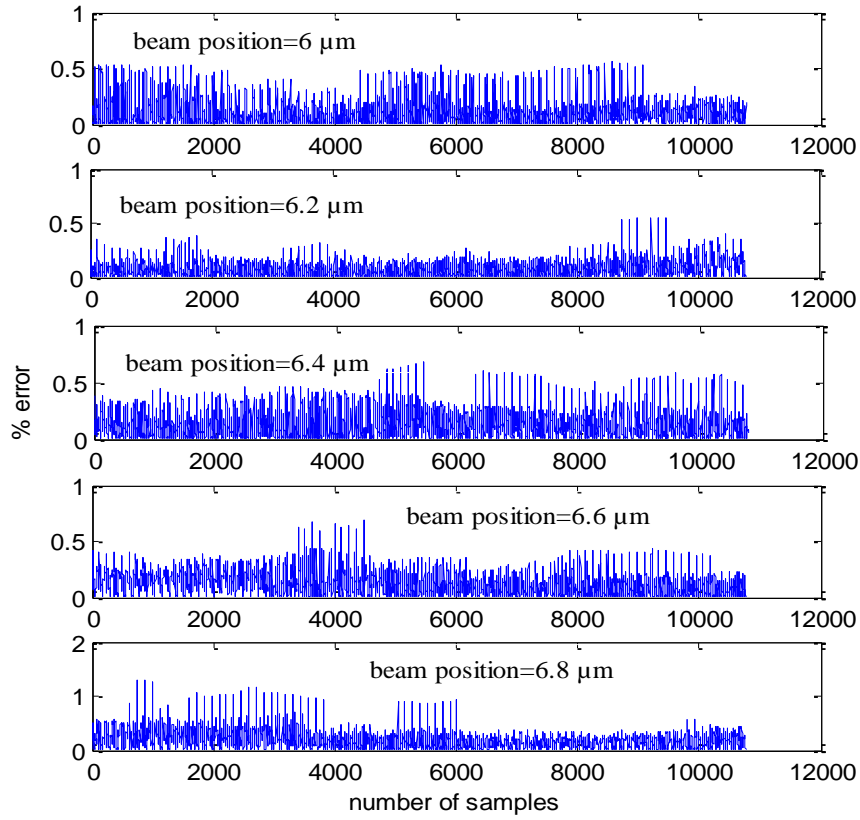


**Fig. 9** Percentage error between the theoretical oversampled EBIC and the oversampled EBIC calculated by ANN

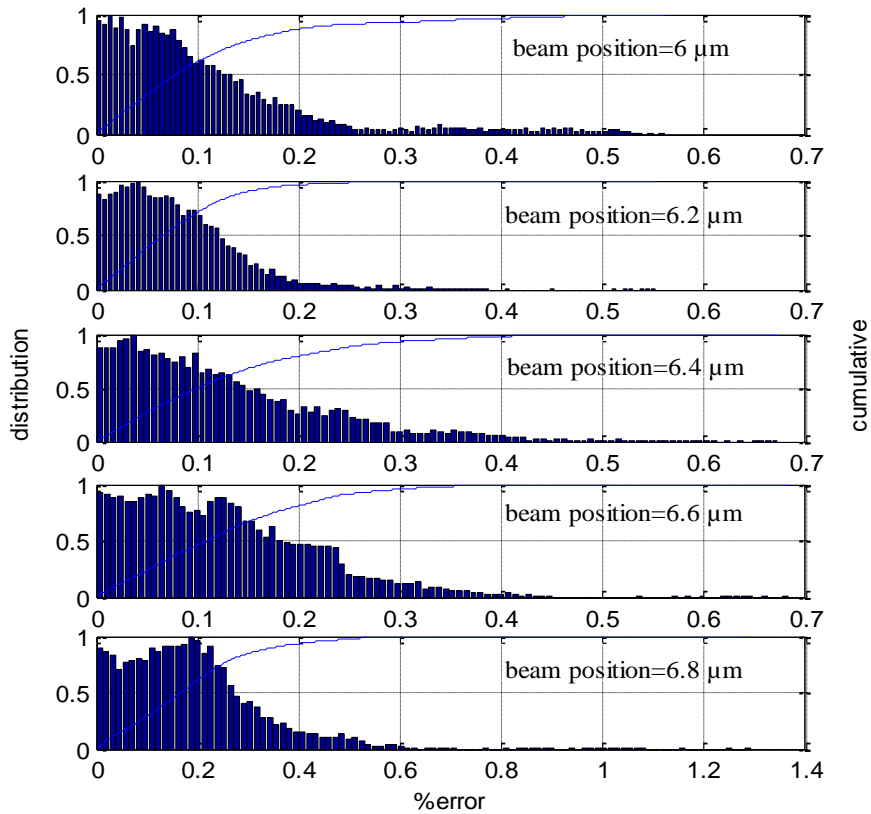


**Fig. 10** PDF and CDF of the percentage error for the oversampled set

**Table 8** Error for 95% and 100% of the oversampled samples

<i>beam position value (<math>\mu\text{m}</math>)</i>	<i>For 95% of the samples, error is below</i>	<i>For 100% of the samples, error is below</i>
6	0.35%	0.55%
6.2	0.2%	0.55%
6.4	0.35%	0.7%
6.6	0.3%	0.7%
6.8	0.45%	1.26%

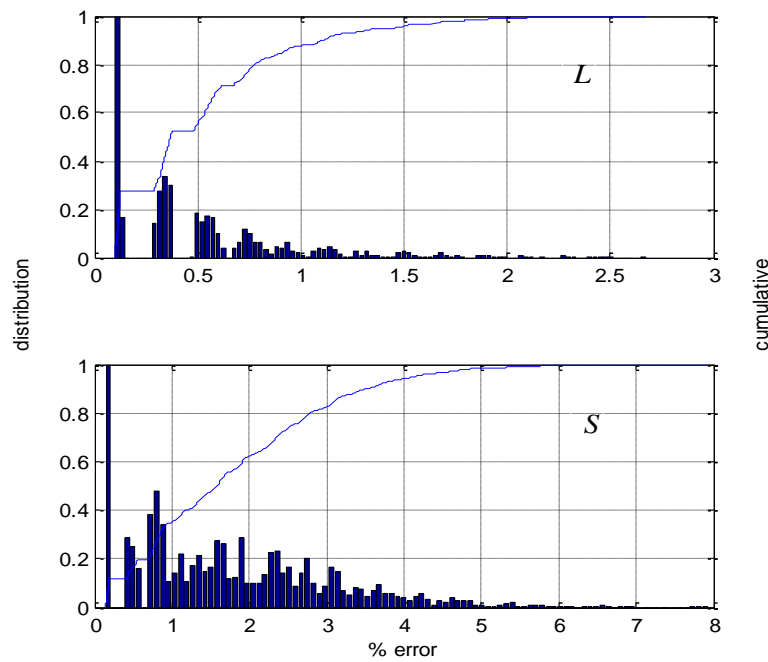


**Fig. 11** PDF and CDF of percentage error of the parameters  $L, S$

**Table 9** Error of the two parameters  $L, S$  for 95% and 100% of the cases

<i>Semiconductor parameter extracted</i>	<i>For 95% of the cases, error is below</i>	<i>For 100% of the cases, error is below</i>
$L (\mu\text{m})$	1.5%	2.7%
$S$	4%	8%

**5. Conclusions**

In this work, we developed a novel method for the simultaneous extraction of the diffusion length and the surface recombination velocity from any theoretically/experimentally obtained EBIC signal. This method is based on neural networks and exhaustive search technique. Simulation results show that a unique set of

parameter values can be obtained with error less than 8% from the true value. This proves the efficiency of the proposed approach.

## References

- [1] I. M. Watt, "The principles and practice of electron microscopy", *Cambridge University Press*, 2<sup>nd</sup> edition 1997
- [2] D. B. Williams, C. B. Carter, "Transmission electron microscopy a textbook for materials science", *Springer* 2<sup>nd</sup> edition 2009.
- [3] S. J. B. Reed, "Electron Microprobe Analysis and Scanning Electron Microscopy in Geology ", *Cambridge University Press* 2<sup>nd</sup> edition 2005.
- [4] L. Reimer, H. Kohl, "Transmission Electron Microscopy, physics of image formation", *Springer* 5<sup>t</sup>.
- [5] H. J. Leamy, "Charge collection scanning electron microscopy", *J. Appl. Phys.*, 53(6), pp. R51-R80. June 1982.
- [6] C. Donolato, "On the Theory of SEM Charge Collection Imaging of Localized Defects in Semiconductors", *Optik* 52(1978/79) No. 1, 19-36.
- [7] A. Jackubowicz, "On the Theory of Electron Beam Induced Current Contrast from Pointlike Defects in Semiconductors", *J. Appl. Phys.*, 57(4), pp. 1194-1199, 15. Feb. 1985.
- [8] A. Jakubowicz, "Theory of Lifetime Measurement With the Scanning Electron Microscope in a Semiconductor Containing a Localized Defect: Transient Analysis", *J. Appl. Phys.* 58(4), pp 1483-1488, 15 August 1985.
- [9] S. Hildebrandt, J. Schreiber, W. Hergert, H. Uniewsk and H. S. Leipner, "Theoretical Fundamentals and Experimental Materials and Defect Studies using Quantitative Scanning Electron Microscopy-Cathodoluminescence/Electron Beam Induced Current on Compound Semiconductors", *Scanning microscopy*, Vol. 12, No. 4, 1998 (pages 535-552).
- [10] D. E. Ioannou and C. A. Dimitriadis, "A SEM-EBIC Minority Carrier Diffusion Length Measurement Technique," *IEEE Trans. Electron Devices*, vol. 29, no. 3, pp. 445450, 1982.
- [11] F. Berz and H. K. Kuiken, "Theory of Life Time Measurements with the Scanning Electron Microscope: Steady state," *Solid State Electronics*, vol. 19, pp. 437445, 1976.
- [12] H. K. Kuiken and C. V. Opdorp, "Evaluation of diffusion length and surface recombination velocity from a planar collector geometry electron beam induced current scan," *J. Appl. Phys.*, vol. 57, no. 6, pp. 2077-2090, 1985.
- [13] C. Donolato, "Charge Collection in a Schottky Diode as a Mixed Boundary Value Problem," *Solid-State Electron.*, vol. 28, no. 11, pp. 1143-1 151, 1985.
- [14] D. E. Ioannou and S. M. Davidson, "Diffusion length evaluation of boron-implanted silicon using the SEM-EBIC/Schottky diode technique," *J. Phys. D: Appl. Phys.*, vol. 12, pp. 1339-1344, 1979.
- [15] D. E. Ioannou, "A SEM-EBIC Minority carrier Lifetime Measurement Technique," *J. Phys. D: Appl. Phys.*, vol. 13, pp. 611-616, 1980.
- [16] D. E. Ioannou and S. M. Davidson, "SEM-EBIC Studies of Boron Implanted Silicon," *J. Micros.*, vol. 118, no. 3, pp. 337-342, 1980.
- [17] S. M. Davidson and C. A. Dimitriadis, "Advances in the Electric Assessment of Semiconductors Using the Scanning Electron Microscope," *J. Micros.*, vol. 118, no. 3, pp. 275-290, 1980.
- [18] C. A. Dimitriadis, "Determination of Bulk Diffusion Length in Thin Semiconductor Layers by SEM-EBIC," *J. Phys. D: Appl. Phys.*, vol. 14, pp. 2269-2274, 1981.
- [19] Daniel S. H. Chan, Vincent K. S. Ong, and Jacob C. H. Phang, "A Direct Method for the Extraction of Diffusion Length and Surface Recombination Velocity from an EBIC Line Scan: Planar Junction Configuration", *IEEE Trans. Electron Devices* , vol. 42, no. 5, MAY 1995.
- [20] Oka Kurniawan and Vincent K. S. Ong, "Determination of Diffusion Lengths With the Use of EBIC from a Diffused Junction With Any Values of Junction Depths", *IEEE Transactions on Electron Devices*, Vol.53, No.9, Sep 2006.
- [21] A. K. Hartmann, H. Rieger, "Optimization algorithms in Physics", Wiley-VCH Verlag Berlin GmbH, Berlin (Federal Republic of Germany), 1<sup>st</sup> edition 2002.
- [22] R. L. Haupt and S. E. Haupt, " Practical Genetic Algorithms", 2<sup>nd</sup> edition, Jhon Wiley and Sons, INC, publications 2004, New Jersey.
- [23] G. L. Tan, S. W. Pan, W. H. Ku, and A. J. Shey, "ADIC-2.C: A General-Purpose Optimization program Suitable for Integrated Circuit Design Applications Using the Pseudo Objective Function Substitution Method (POSM)", *IEEE Transactions on computer aided design*, Vol. 1, No. 11, pp. 1150-1163, Nov 1988.
- [24] M. I. Lourakis, A. A. Argyros, "Is Levenberg-Marquardt the most efficient optimization algorithm for implementing bundle adjustment", *Proceeding of the Tenth IEEE international conference on computer vision*, Vol. 2, pp. 1526-1531. 2005.
- [25] S. Haykin, "Neural Networks; A Comprehensive Foundation", Prentice Hall; 2 edition, 1999.
- [26] D. Busuioc, "Circuit model parameter extraction and optimization for microwave filters", master thesis, university of waterloo, Ontario, Canada 2002.

- [27] L. Cazzanty, M. Khan, F. Cerrina, "Parameter extraction with neural networks", Proc. SPIE, Vol.3332, 654 (1998), online publication. 5 june 2003.
- [28] Avitabile, G. Chellini, B. Fedi, A. Luchetta, S. Manetti, "A neural architecture for the parameter extraction of high frequency devices" Circuits and Systems, ISCAS May 2001. *IEEE International Symposium*, pp 577 – 580, vol. 2.
- [29] A. Caddemi, and N. Donato, "Advanced Simulation of Semiconductor Devices by artificial neural networks", *Journal of computational electronics 2*: 301-307, 2003.
- [30] H. Taher, D. Schreurs, and B. Nauwelaers, "Extraction of Small Signal Equivalent Circuit Model parameter for statistical modeling of HBT using artificial neural", *13<sup>th</sup> GAAS Symposium-Paris*, 2005.
- [31] B. Rajendran, "Modeling of SiGe heterostructure pMOSFET devices using neural networks", Bachelor of technology thesis, Indian institute of technology, Kharagpur, May 2000.
- [32] T. Zahradnicky, "MOSFET parameter extraction", dissertation thesis proposal, Czech Technical University in Prague, Sep 2005.
- [33] M. G. Xibilia, "Advanced Simulation of Semiconductor Devices by artificial neural networks", *journal of computational electronics 2*: 301-307, 2003.
- [34] Reimer, "Scanning Electron Microscopy physics of image formation and microanalysis", Springer 2<sup>nd</sup> edition 1998.
- [35] Donolato, "On the Analysis of Diffusion Length Measurements by SEM", *Solid State Electronics*, Vol. 25, No. 11, pp. 1077-1081, 1982.
- [36] Oka. Kurniawan, "Device Parameters Characterization With the Use of EBIC", a thesis submitted for the degree of *Doctor of Philosophy*, Nanyang Technological University, 2008, supervised by Professor V. K. S. Ong.
- [37] Kurniawan. O, Ong. K. S, "Choice of Generation Volume Models for Electron Beam Induced Current Computation", *IEEE Transactions on Electron Devices* 56(5), 1094-1099, 2009.